A UNITED STATES DEPARTMENT OF COMMERCE PUBLICATION

ESSA Technical Report ERL 163-ITS 105

U.S. DEPARTMENT OF COMMERCE
Environmental Science Services Administration
Research Laboratories

Ground Wave Propagation in an Ionized Atmosphere With Arbitrary Variation of the Conductivity With Altitude

J. RALPH JOHLER

BOULDER, COLO.
MARCH 1970

ESSA RESEARCH LABORATORIES

The mission of the Research Laboratories is to study the oceans, inland waters, the lower and upper atmosphere, the space environment, and the earth, in search of the understanding needed to provide more useful services in improving man's prospects for survival as influenced by the physical environment. Laboratories contributing to these studies are:

Earth Sciences Laboratories: Geomagnetism, seismology, geodesy, and related earth sciences; earthquake processes, internal structure and accurate figure of the Earth, and distribution of the Earth's mass.

Atlantic Oceanographic and Meteorological Laboratories and Pacific Oceanographic Laboratories: Oceanography, with emphasis on ocean basins and borders, and oceanic processes; sea-air interactions: and land-sea interactions. (Miami, Florida)

Atmospheric Physics and Chemistry Laboratory: Cloud physics and precipitation; chemical composition and nucleating substances in the lower atmosphere; and laboratory and field experiments toward developing feasible methods of weather modification.

Air Resources Laboratories: Diffusion, transport, and dissipation of atmospheric contaminants; development of methods for prediction and control of atmospheric pollution. (Silver Spring, Maryland)

Geophysical Fluid Dynamics Laboratory: Dynamics and physics of geophysical fluid systems; development of a theoretical basis, through mathematical modeling and computer simulation, for the behavior and properties of the atmosphere and the oceans. (Princeton, New Jersey)

National Severe Storms Laboratory: Tornadoes, squall lines, thunderstorms, and other severe local convective phenomena toward achieving improved methods of forecasting, detecting, and providing advance warnings. (Norman, Oklahoma)

Space Disturbances Laboratory: Nature, behavior, and mechanisms of space disturbances; development and use of techniques for continuous monitoring and early detection and reporting of important disturbances.

Aeronomy Laboratory: Theoretical, laboratory, rocket, and satellite studies of the physical and chemical processes controlling the ionosphere and exosphere of the earth and other planets.

Wave Propagation Laboratory: Development of new methods for remote sensing of the geophysical environment; special emphasis on propagation of sound waves, and electromagnetic waves at millimeter, infrared, and optical frequencies.

Institute for Telecommunication Sciences: Central federal agency for research and services in propagation of radio waves, radio properties of the earth and its atmosphere, nature of radio noise and interference, information transmission and antennas, and methods for the more effective use of the radio spectrum for telecommunications.

Research Flight Facility: Outfits and operates aircraft specially instrumented for research; and meets needs of ESSA and other groups for environmental measurements for aircraft. (Miami, Florida)

ENVIRONMENTAL SCIENCE SERVICES ADMINISTRATION

BOULDER, COLORADO 80302

U. S. DEPARTMENT OF COMMERCE
Maurice H. Stans, Secretary

ENVIRONMENTAL SCIENCE SERVICES ADMINISTRATION
Robert M. White, Administrator

RESEARCH LABORATORIES
Wilmot N. Hess, Director

ESSA TECHNICAL REPORT ERL 163-ITS 105

Ground Wave Propagation in an Ionized Atmosphere With Arbitrary Variation of the Conductivity With Altitude

J. RALPH JOHLER

INSTITUTE FOR TELECOMMUNICATION SCIENCES
BOULDER, COLORADO
March 1970

For sale by the Superintendent of Documents, U. S. Government Printing Office, Washington, D. C. 20402
Price 35 cents.

FOREWORD

The mathematical techniques presented in this paper were developed for the Defense Atomic Support Agency as part of the work performed under interagency work order 804-69. This paper deals with the specific task of estimating arbitrary altitude variations in the ion content of the atmosphere in the nuclear environment and of developing mathematical techniques for calculating ground waves in such an environment.

The listing of the FORTRAN computer program is available from the author upon request.

TABLE OF CONTENTS

ABSTRACT

The atmosphere can apparently be ionized to such a degree that the ground wave is disturbed, as a result of, for example, a nuclear event, and ionizing radiation of sufficient intensity to overcome the ion-ion recombination processes may cause the ions to accumulate near the surface of the ground. Gamma radiation from the fallout of a nuclear weapon may produce such ionization for a considerable time after the nuclear event. The problem is similar to that of terrestrial radio wave propagation via the ionosphere, except that in the former case the ionization has a maximum near the surface of the ground and decreases exponentially with altitude. In other words, we have an upside down ionosphere to consider. A new theoretical approach to such ground wave problems based on methods of numerical analysis has been developed for computer application. The computer computation concept is discussed, and sample computations based on the fallout model profile are presented. A particular fallout model based on data given in the U. S. Atomic Energy Commission's handbook on "The Effects of Nuclear Weapons" is considered in some detail, and the effect of an ionization profile (ion number density as a function of altitude) on the propagation of the ground wave is ascertained. A physically possible but not likely extra attenuation of 12 dB at 100 km distance is noted.

GROUND WAVE PROPAGATION IN AN IONIZED ATMOSPHERE WITH ARBITRARY VARIATION OF THE CONDUCTIVITY WITH ALTITUDE

J. Ralph Johler

1. INTRODUCTION

In an earlier paper (Johler, 1969a) ground wave propagation in a uniformly ionized atmosphere was considered in some detail. It was found that uniform ionization of the atmosphere in the vertical direction could affect ground wave propagation if the ionization were sufficiently intense. Some nuclear events apparently provide sources which could cause a disturbance of the ground wave. In this paper, we take a more realistic and more complicated approach by introducing a profile or variation of the atmospheric conductivity with altitude. For example, gamma radiation from the fallout of a nuclear weapon may produce intense ionization near the surface of the ground for a considerable time after the nuclear event. The ionization will decrease rapidly with altitude. This problem is similar to that of terrestrial radio wave propagation via the ionosphere, but in the latter case the ionization has a maximum near the surface of the ground and decreases approximately exponentially with altitude. Thus fallout produces an upside-down ionosphere.

The basic unit for measuring fallout (AEC, 1962, p.375) is the roentgen, which is the quantity or "dose" of gamma radiation or x-rays that will give rise to $2.08(10^9)$ ion pairs/cc under standard atmospheric conditions at sea level. An interesting case is cited by AEC (1962, p.462), which gives the radiation level for the BRAVO test explosion (15 Mt yield). At a distance of 190 km and a time of 96 hours after the explosion, the level of 3000 roentgens was noted. The roentgen can be converted into an average production rate,

$$q = \frac{\text{roentgens}}{\text{time}}\ 2.08(10^9) = \frac{\text{roentgens}}{98 \times 3600}\ 2.08(10^9)\ \text{ions/cc/sec.} \qquad (1.1)$$

The unit dose rate may be greater than the average does rate. Referring again to AEC (fig. 920, p.423), we can conclude that the production rate q should be increased by a factor of 96/ 8.2, or approximately 12. Thus the unit time dose rate deduced from 3000 roentgens at 96 hours is 3000/ 8.2, or 366 roentgens per hour at one 1 hour and 1.5 roentgens per hour at 96 hours. The average dose rate is, of course, between these values or 3000/ 96 or 31.25 roentgens per hour. (For references of this type see AEC, fig. 9.16a). The profile in figure 1, which is based on figure 9.181 in the AEC handbook, gives the dose rate variation with altitude of a uniform distribution of radiation sources over an infinite plane. Thus a profile of ion density and conductivity as a function of altitude can be deduced from the formulas

$$N_+ = \sqrt{\frac{q}{\alpha_i}}\ , \qquad (1.2)$$

and

$$\sigma = 2\,\frac{e^2}{m_+}\,\frac{N_+}{\nu_{+,o}\,\epsilon_o}\,\frac{m_+ + m_o}{m_o}\ . \qquad (1.3)$$

Here, e^2/m_+ is the ratio of electronic charge squared to the mass of the positive ion. The permittivity is given by $\epsilon_o \sim 8.85419(10^{-12})$, and the positive ion-neutral collision frequency $\nu_{+,o}$ is given in figure 1. The collision frequency $\nu_{+,o}$ is multiplied by the mass ratio of neutral mass m to the sum of positive ion and neutral mass to account for the redistribution of velocity after collision (Johler and Berry, 1965). This point is often overlooked because, in the case of electron-neutral

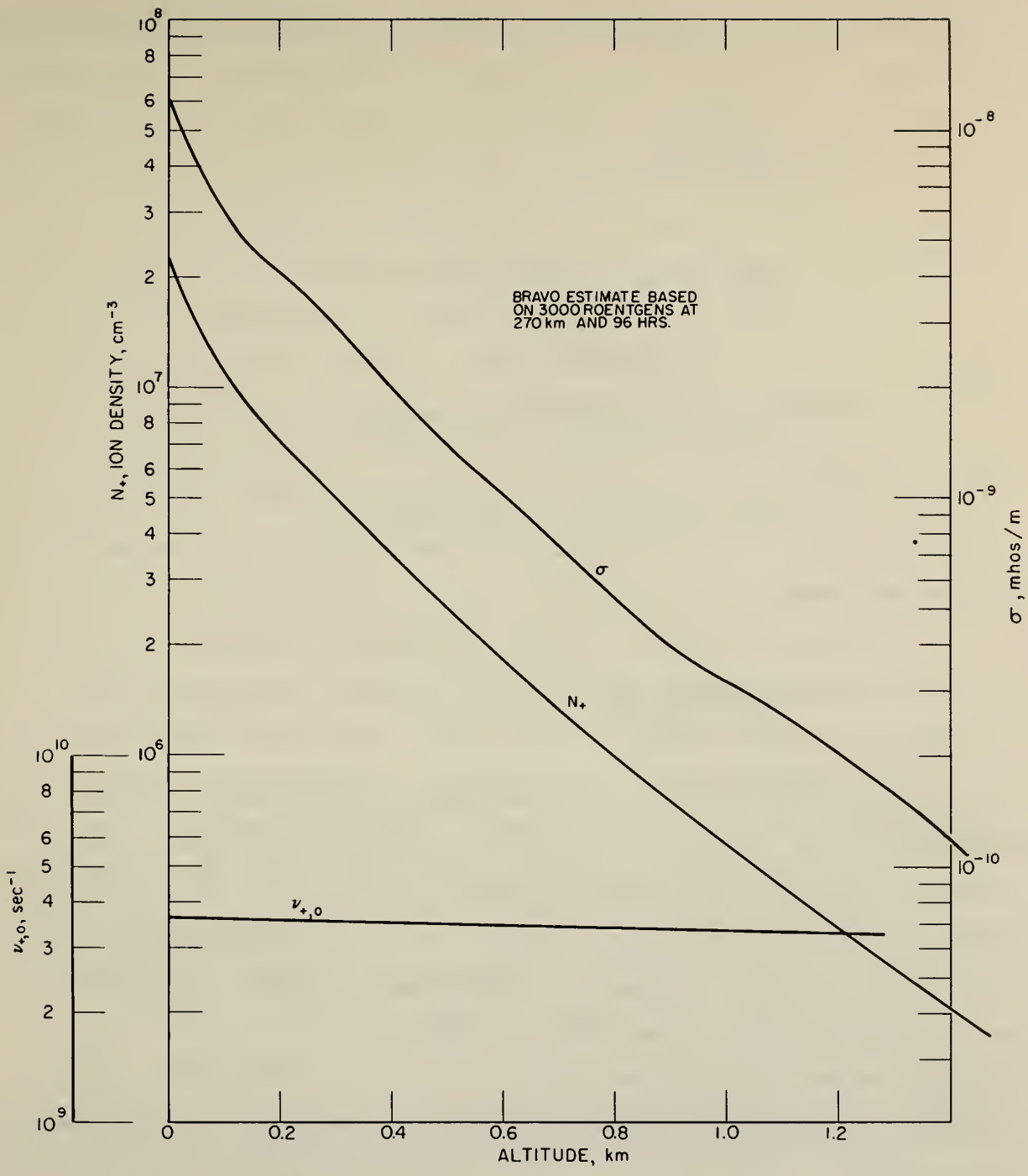

Figure 1. Theoretical profile of atmospheric conductivity, positive ion density, and collision frequency. Ion densities are based on fallout measurements 270 km from ground zero and 96 hours after the BRAVO nuclear test. This is the case $F_n = 1$, with an average dose rate and a nominal ion-ion recombination coefficient $\alpha_{1,0} \sim 3(10^{-8})$.

collisions, the mass ratio times the collision frequency in the hydrodynamic equation is

$$\frac{m_o}{m_e + m_o} \nu_{e,o} \sim \nu_{e,o} ,$$

since

$$m_e << m_o .$$

Thus,

$$m_o \sim 5.313(10^{-26}) \text{ for oxygen,}$$

and

$$m_e \sim 9.108(10^{-31}) \text{ in kilograms.}$$

On the other hand,

$$\frac{m_o}{m_+ + m_o} \nu_{+,o} = \frac{1}{2} \nu_{+,o} ,$$

if we assume positive ions and neutrals have the same mass. Thus, strictly speaking, the effective collision frequency is half the actual collision frequency in the case of ion-ion collisions in which each of the colliding particles have the same mass. This means that the drift velocity change after a collision is redistributed equally between the two colliding particles. Since the ion collision frequency is now more precisely known, the mass ratio described above should be taken into account in the equation of motion of the ions, as was done by Johler and Berry (1965).

The conductivity σ reflects the effect of the mass ratio on the resultant ion velocity change. The number density N_+ is critically dependent upon the value of the ion-ion recombination rate, α_i cm^3 / sec, near the ground. Considerable uncertainty as to the value of α_i seems

to exist in the literature. The lowest possible value is the two-body ion-ion recombination rate used at high altitude, $\alpha_i \sim 3(10^{-8})$ (Knapp, 1969, private communication, G.E. Tempo, Santa Barbara, California); the highest value quoted for the three-body ion-ion recombination rate is $\alpha_i \sim 3(10^{-6})$. This difference, by a factor of 100, between these values means that the profile in figure 1 would change from one that would have little effect on the propagation of the ground wave to one that would seriously alter it. Until recently the three-body ion-ion recombination rate most quoted in the literature $\alpha_i \sim 2.65(10^{-6})$ (see, for example, Loeb, 1961) was apparently based on researches by Thomson (1906, 1924), Thomson and Thomson (1933), Rutherford (1913) and Natanson (1959). Experimental verification of the theory by Sayers (1938) gave the value quoted above, which agreed with theory. More recently, Bruechner (1964) quotes a value of $3.95(10^{-7})\text{cm}^3/\text{sec}$ for α_i. This is based on a corrected theory of ion-ion recombination that accounts for an error in the Thomson-Natanson theory by retaining the more rigorous expression for the value of the average energy in the analysis. Brueckner concludes: "The disagreement (with the Thomson-Natanson theory) may be due to the simplifying assumptions of the Thomson theory as modified in this paper to include dissociative collisions, such as the failure to consider the internal degrees of freedom of the ions and the dispersion in energy and momenta of the colliding particles. The changes which result from a more complete theory than previously used suggest, however, that the previous agreement between theory and experiment has been fortuitous". More recently experimental evidence has been obtained in support of Brueckner's theory (Hirsh, 1967), indicating that a considerably lower value of α_i should be used near the ground.

Taking into account the uncertainty in α_i and the production rate q, we can translate the profile shown in figure 1 simply by using an ion number density multiplication factor F_n. Thus a change in the

production rate or the ion-ion recombination rate merely modifies the number density N_+ in (1.2). Physically possible values, according to this author's estimates, range from $F_n = 0.1$ to $F_n = 20$ in a nuclear environment. This would correspond to ground level production rates $q/q_o = 0.01$ to 400, where q_o is the average production rate for the BRAVO profile (fig. 1). Thus, in the lower limit, $F_n = 0.1$, the techniques described in this paper recovered the numerical values calculated from the classical ground wave theory within a fraction of a decibel in the amplitude at a frequency of 100 kHz and distances of 100 km or less. The particular case of BRAVO given by AEC would be represented approximately by $F_n = 1$ or 2, depending on the time. Therefore, (1.2) becomes

$$N_+ = F_n \sqrt{\frac{q_o}{\alpha_{i,o}}} \quad , \tag{1.4}$$

where

$$q_o = 1.8(10^7) \quad , \tag{1.5}$$

and

$$\alpha_{i,o} = 3(10^{-8}) \quad . \tag{1.6}$$

This paper solves the electromagnetic theory problem of a ground wave signal propagating from an electrical point source dipole to distances less than approximately 300 km and over finitely conducting ground with an arbitrary variation with altitude of the conductivity of the atmosphere. Numerical values for F_n between 0.1 and 40 are considered at a frequency of 100 kHz.

2. THEORETICAL CONSIDERATIONS

The problem of ground wave propagation at medium and low frequencies in an ionized atmosphere ordinarily concerns short distances, say, 50 to 100 km. It is therefore more practical from a theoretical point of view to regard the earth as flat and solve the problem in terms of a Cartesian coordinate system.

An ionized atmosphere can be accommodated in the analysis of the ground wave with a system of boundary conditions as depicted in figure 2. Thus, the profile in figure 1 is approximated as a function of altitude with a set of plasma slabs. This is the method used by Johler and Harper (1962). At the low altitudes that pertain to the ground wave, atmospheric reflections are a consequence of the presence of ions that exhibit isotropic behavior at medium and low frequencies. Therefore, advantage can be taken of the simplification resulting from zero terrestrial magnetic field. A detailed treatment of the effects of ions is discussed in an earlier paper (Johler and Berry 1965).

The scheme for calculating the reflection process is depicted in figure 2. Each slab of the system of slabs contains a reflection coefficient T_i at the top, a reflection coefficient R_i at the bottom, and a transmission coefficient U_i connecting it to the adjacent slab. As the thickness of each slab Z_i is decreased and the number p of slabs is increased, convergence can be obtained on a reflection coefficient $T_{\bullet\bullet}$. The phase of the reflection coefficient $T_{\bullet\bullet}$ is referenced to the height h. This reflection coefficient is a function of the slab reflection and transmission coefficients T_i, R_i, U_i, and T within the system of slabs. The first slab of thickness h contains the source dipole and hence must be treated separately to accommodate the spherical waves emanating from such an electrical point source. The analysis presented below then relates the bottom of the slab system at height h (fig. 2) to the ground and to a source dipole (transmitter).

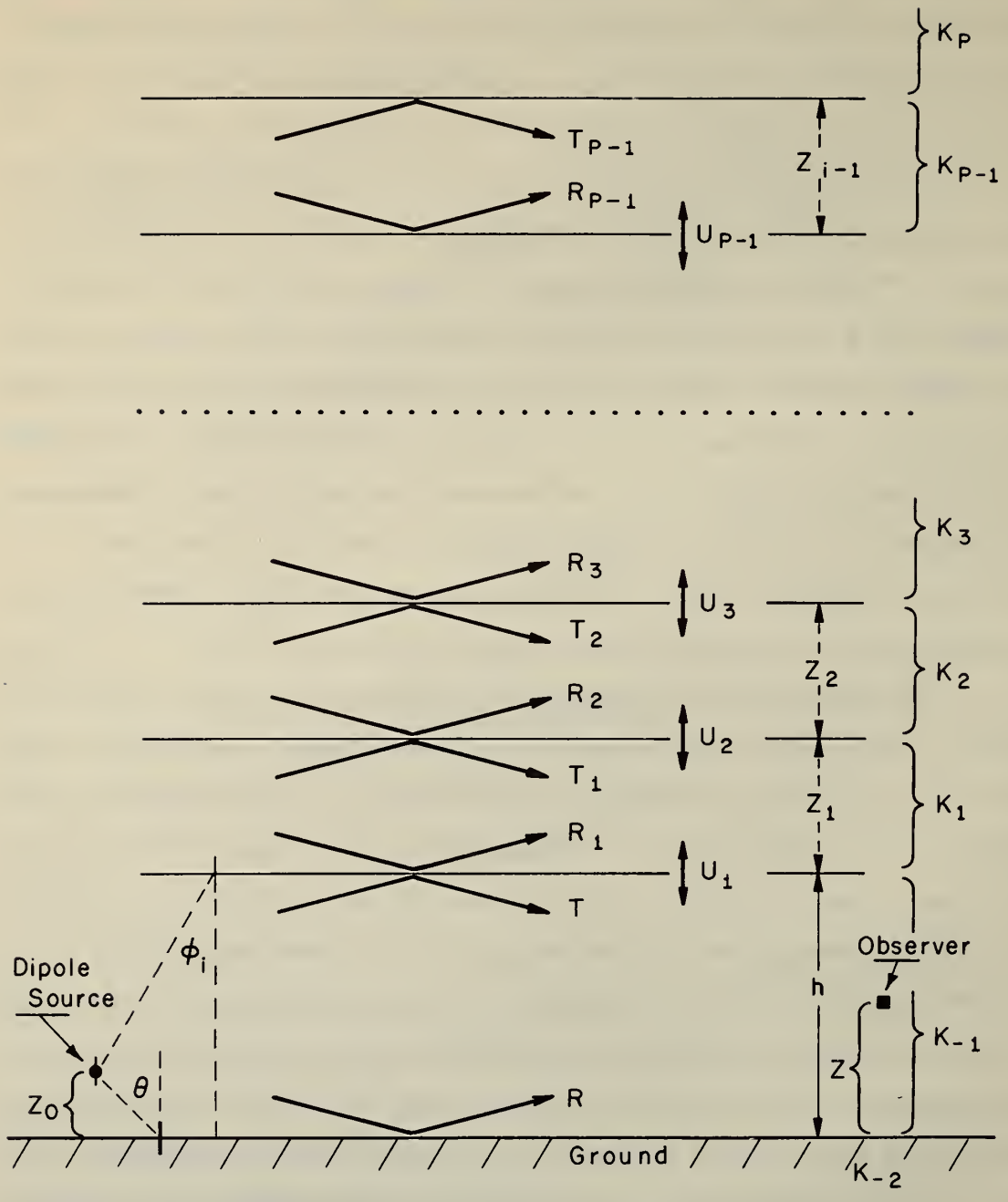

Figure 2. Theoretical treatment of the profile based on the concept of continuous stratification of the altitude variation of a atmospheric ion content or conductivity.

The reflection coefficient $T_{\cdot\cdot}$ implies vertically polarized waves characteristic of a vertical electric dipole source. A similar reflection coefficient T_{mm}, for horizontal dipole sources could also be used. Finally, since an isotropic ionosphere is assumed, the abnormal components given by Johler and Harper (1962) are zero ($T_{\cdot m} = T_{m\cdot} = 0$).

If θ (fig. 2) or φ_1 is an angle of incidence for a single semi-infinite slab, then

$$T_{\cdot\cdot} = \frac{\cos\theta - \frac{k_{-1}}{k_1}\sqrt{1 - \left(\frac{k_{-1}}{k_1}\sin\theta\right)^2}}{\cos\theta + \frac{k_{-1}}{k_1}\sqrt{1 - \left(\frac{k_{-1}}{k_1}\sin\theta\right)^2}} \quad . \tag{2.1}$$

Similarily, the ground reflection coefficient for vertical polarization can be written

$$R_e = \frac{\cos\theta - \frac{k_{-1}}{k_{-2}}\sqrt{1 - \left(\frac{k_{-1}}{k_{-2}}\sin\theta\right)^2}}{\cos\theta + \frac{k_{-1}}{k_{-2}}\sqrt{1 - \left(\frac{k_{-1}}{k_{-2}}\sin\theta\right)^2}} \quad . \tag{2.2}$$

The wave number of the ground, assumed to be of infinite extent in the negative z-direction (fig. 2) can be written

$$k_{-2} = \frac{\omega}{c}\sqrt{\epsilon_2 - i\frac{\sigma}{\epsilon_o \omega}} \quad , \tag{2.3}$$

where ϵ_2 and σ are the dielectric constant and conductivity of the ground, respectively. The frequency f is given by $f = \omega/2\pi$ (hertz). The speed of light is $c \sim 2.997925(10^8)$m/s, and ϵ_o is the permittivity of space, $\epsilon_o = 8.(10^{-12})$. In a particular slab along the profile,

$$k_i = \frac{\omega}{c}\sqrt{1 - i\frac{\sigma_i}{\epsilon_o \omega}} \quad , \tag{2.4}$$

where

$$\sigma_i = \frac{N_e e^2}{m_e(\nu'_{e,o} + i\omega)} + \frac{N_+ e^2}{m_+(\nu'_{+,o} + i\omega)} + \frac{N_- e^2}{m_-(\nu'_{-,o} + i\omega)} \quad , \tag{2.5}$$

$$\nu'_{a\,o} = \frac{m_o}{m_a + m_o} \quad , \quad a = e, +, - \quad ,$$

and where the ratio of charge squared of the electron, e, to m (m_e, or for the ion $m_{+,-}$), is given by

$$\frac{e^2}{m_e} = 2.8178(10^{-8}) \qquad \text{(for electrons)} \quad ,$$

and

$$\frac{e^2}{m_+} = 4.8310(10^{-12}) \qquad \text{(for ionized oxygen)} \quad .$$

Thus, the number densities N_e, N_+, and N_- depend upon the ionizing sources. At the very low altitudes that pertain to the ground wave, the electrons can be neglected, and the positive ions (profile illustrated in fig. 1) provide the important contribution to the finite conductivity of the atmosphere. The appropriate collision frequency as a function of altitude for use in the conductivity calculation is also given in figure 1 as a function of altitude.

Since the bottom slab of wave number k_{-1} contains the source of spherical waves, the propagation in this slab is not as simple. Sommerfeld (1909, 1926) and Weyl (1919), and more recently Brekhovskikh (1960), quickly recognized that the ground wave emanating as a spherical wave from an electrical point source can be expressed as a sum of plane homogeneous waves and plane inhomogeneous waves that could be conveniently used to satisfy the boundary condition for the spherical wave both at the source and at the plane boundaries illustrated in figure 2.

Thus it is not necessary here to make approximations for the boundary conditions at the source as is often done in mode theory (see Budden, 1961, for an extensive treatment of excitation factors for modes). Based on Sommerfeld's (1909) basic approach all waves emanating from the dipole can be included in the analysis. This is especially important in dealing with the problem of the ionized atmosphere or where the ionosphere is depressed abnormally.

For convenience, let $\beta = k_{-1}$, the wave number of the lowest plasma slab that contains the source and the observer, as shown in figure 2. It is well known that the vertical electric field E_z, for example, can be calculated from the Hertz vector for a vertical dipole source given by

$$\vec{z}\ \Pi_z^e = \left[\frac{i\omega I_o \ell \mu_o c}{-4\pi i \beta} \right] \frac{\exp(-i\beta D)}{D} \vec{z} \qquad (2.6)$$

by the operation

$$E_z = \left[\beta^2 + \frac{\partial^2}{\partial z^2} \right] \Pi_z^e \quad , \qquad (2.7)$$

where

$$D^2 = x^2 + y^2 + z^2 = r^2 + z^2 \ , \qquad (2.8)$$

and where $I_o \ell$ is the dipole current moment in ampere-meters, and μ_o is the permeability, $\mu_o = 4\pi(10^{-7})$ henry/m, and $\vec{z}$ is the unit vector in the z-direction.

The factor $\exp(-i\beta D)/D$ can be written as a Fourier integral to show the equivalent plane wave structure of the spherical wave source:

$$\frac{\exp(-i\beta D)}{D} = \frac{-i}{2\pi} \int_{-\infty}^{\infty} \int_{-\infty}^{\infty} \exp[-i(\beta_x x + \beta_y y + \beta_z z)] \frac{d\beta_x\, d\beta_y}{\beta_z} , \quad (2.9)$$

where

$$\beta_z = [\beta^2 - \beta_x^2 - \beta_y^2]^{\frac{1}{2}} , \quad (2.10)$$

and

$$\beta_x = \beta \sin\theta \cos\varphi ,$$
$$\beta_y = \beta \sin\theta \sin\varphi ,$$
$$\beta_z = \beta \cos\theta ,$$

where θ and φ are the vertical and horizontal spherical coordinate angles respectively. Bessel's function of argument z and order 0 can be written

$$J_o(z) = \frac{1}{2\pi} \int_0^{2\pi} \exp[\pm i z \cos(\varphi - \varphi_i)]\, d\varphi \quad . \quad (2.11)$$

Neglecting the reflections from regions above the source, ($T_{..} = 0$ in fig. 2), one then finds after considerable ado the integral form of the ground wave (see, for example, Brekhovskikh 1960, pp. 242-244 for integrals of this type) to be

$$E_z = \left[-\beta^2 I_o \ell \frac{\mu_o c}{4\pi}\right] \int_0^{\frac{\pi}{2}+i\infty} J_o(\beta r \sin\theta) \left\{\exp[-i\beta(z-z_o)\cos\theta]\right.$$
$$\left. + R_e(\theta) \exp[-i\beta(z+z_o)\cos\theta]\right\} \sin^3\theta\, d\theta \quad . \quad (z \geq z_o) \quad (2.12)$$

The integration contour is taken from 0 to $\pi/2$ and thence from $\pi/2$ to the infinity of the imaginary axis. It is apparent that the solution can

be split into two integrals: (a) the finite integral from 0 to $\pi/2$ comprising the homogeneous plane waves and (b) the infinite integral from $\pi/2$ to $i\infty$ comprising the inhomogeneous plane waves. Thus,

$$E_z = \left[-\beta^2 I_o \ell \frac{\mu_o c}{4\pi} \right] \int_o^{\frac{\pi}{2}} \left\{ \exp\left[-i\beta (z - z_o) \cos\theta \right] \right.$$

$$\left. + R_e \exp\left[-i\beta (z + z_o) \cos\theta \right] \right\} J_o(\beta r \sin\theta) \sin^3\theta \, d\theta$$

$$+ \left[-i\beta^2 I_o \ell \frac{\mu_o c}{4\pi} \right] \int_o^{\infty} \left\{ \exp\left[-\beta (z - z_o) \sinh\theta \right] \right.$$

$$\left. + R'_e \exp\left[-\beta (z + z_o) \sinh\theta \right] \right\} J_o(\beta r \cosh\theta) \cosh^3\theta \, d\theta \quad (z \geq z_o) \,, \tag{2.13}$$

where, in the second integral,

$$R'_e(\theta) = \frac{-i \sinh\theta - \frac{k_{-1}}{k_{-2}} \sqrt{1 - \left(\frac{k_{-1}}{k_{-2}} \cosh\theta \right)^2}}{-i \sinh\theta + \frac{k_{-1}}{k_{-2}} \sqrt{1 - \left(\frac{k_{-1}}{k_{-2}} \cosh\theta \right)^2}} \,. \tag{2.14}$$

The height of the transmitter z_o or the receiver z above ground appears in the exponential functions, where it is assumed $z \geq z_o$. The second integral is the most difficult to evaluate, but it converges primarily as a consequence of the exponential functions. In fact, the greater the altitude of the receiver, the more rapid the convergence. As the receiver altitude is reduced to zero, if the transmitter altitude is assumed to be zero, the computation depends upon the Bessel function $J_o(z)$ for convergence.

If we assume that the complete reflection coefficient $T_{\bullet\bullet}$ at the top of the bottom slab in figure 1 has been evaluated, $T_{\bullet\bullet} = F(T, T_1, R_1 U_1, T_2, R_2, U_2 \cdots)$. Assigning the appropriate ion density to $\beta = k_{-1}$ (thus β may be a complex number), we can obtain the complete solution to the problem by analogy to ground wave theory (2.13):

$$E_z = \left[-\beta^2 I_o \ell \frac{\mu_o c}{4\pi} \right] \int_0^{\frac{\pi}{2}} \left\{ \exp\left[-i\beta(z-z_o)\cos\theta\right] \right.$$

$$+ R_\bullet \exp\left[-i\beta(z+z_o)\cos\theta\right] + T_{\bullet\bullet} \exp\left[-i\beta(2h-z-z_o)\cos\theta\right]$$

$$\left. + R_\bullet T_{\bullet\bullet} \exp\left[-i\beta(2h-z+z_o)\cos\theta\right] \right\} \left\{ 1 - R_\bullet T_{\bullet\bullet} \exp(-2i\beta h\cos\theta) \right\}^{-1}$$

$$\times J_o(\beta r \sin\theta) \sin^3\theta \, d\theta$$

$$+ \left[-i\beta^2 I_o \ell \frac{\mu_o c}{4\pi} \right] \int_0^{\infty} \left\{ \exp\left[-\beta(z-z_o)\sinh\theta\right] \right.$$

$$+ R'_\bullet \exp\left[-\beta(z+z_o)\sinh\theta\right] + T'_{\bullet\bullet} \exp\left[-\beta(2h-z-z_o)\sinh\theta\right]$$

$$\left. + R'_\bullet T'_{\bullet\bullet} \exp\left[-\beta(2h-z+z_o)\sinh\theta\right] \right\} \left\{ 1 - R'_\bullet T'_{\bullet\bullet} \exp(-2\beta h \sinh\theta) \right\}^{-1}$$

$$\times J_o(\beta r \cosh\theta) \cosh^3\theta \, d\theta \quad , \qquad (z \geq z_o) \qquad (2.15)$$

where $R_\bullet$ and $R'_\bullet$ are given by (2.2) and (2.14) respectively. For a single semi-infinite slab, $T_{\bullet\bullet}$ is given by (2.1), and $T'_{\bullet\bullet}$ can be written

$$T''_{\bullet\bullet} = \frac{-i\sinh\theta - \frac{k_{-1}}{k_1}\sqrt{1-\left(\frac{k_{-1}}{k_1}\cosh\theta\right)^2}}{-i\sinh\theta + \frac{k_{-1}}{k_1}\sqrt{1-\left(\frac{k_{-1}}{k_1}\cosh\theta\right)^2}} \quad . \tag{2.16}$$

The second integral representing the inhomogeneous waves converges for the same reasons as in the case of the ground wave (2.13). In the complex z-plane, $J_o(z)$ grows without bounds and may cause the second integral (2.15) to diverge if Im z is sufficiently great to overcome the exponential functions. This requires a shift of the integration contour to keep the argument z of $J_o(z)$ real. Thus, if

$$z\cosh\xi = (x+iy)\cosh\theta = A\exp(i\varphi)\cosh\theta \ , \tag{2.17}$$

the required integration contour of the second integral (2.15) in its complex $\xi = \xi' + i\xi''$ plane is given by

$$\xi' + i\xi'' = \cosh^{-1}\{\exp(-i\varphi)\cosh\theta\} \ , \tag{2.18}$$

$$\xi' + i\xi'' = \ln\{\exp(-i\varphi)\cosh\theta + \sqrt{\exp(-2i\varphi)\cosh^2\theta - 1}\} \ , \tag{2.19}$$

provided that

$$d(\xi' + i\xi'') = \left[\frac{\exp(-i\varphi)\sinh\theta}{\sqrt{\exp(-2i\varphi)\cosh^2\theta - 1}}\right] d\theta \quad . \tag{2.20}$$

The integration contour then passes from zero to the point P_1 in figure 3. At P_1,

$$\theta = \theta_1' + i\theta_1'' \ ,$$

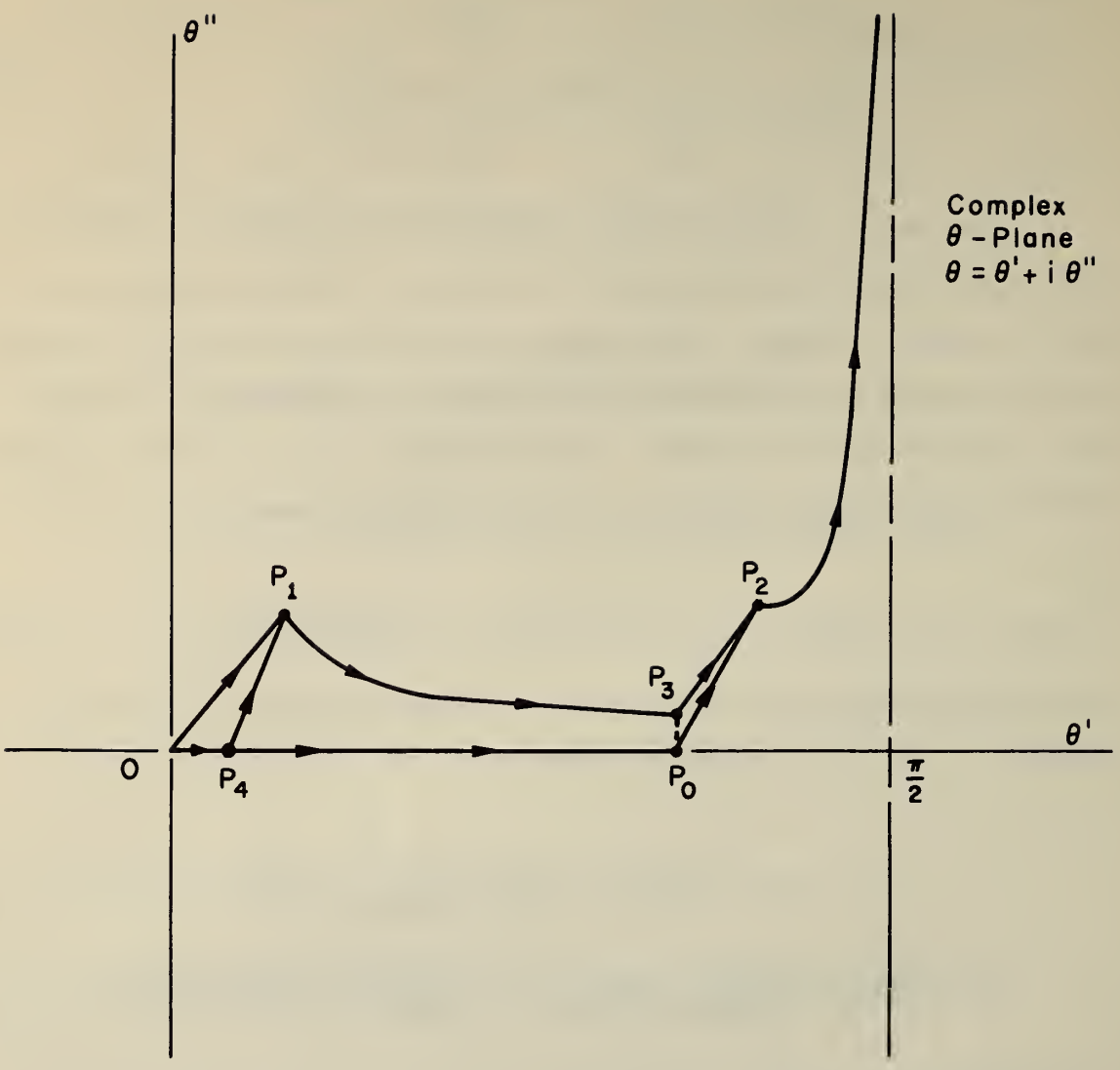

Figure 3. Map of complex θ-plane, illustrating integration contour.

where we may choose

$$\theta_1' + i\theta_1'' = \ell n \left[\exp(-i\varphi) + \sqrt{\exp(-2i\varphi) - 1}\,\right]$$

$$= \cosh^{-1}[\exp(-i\varphi)] .$$

The contour path is then from P_1 to P_3, where, at P_3, $\theta_3' + i\theta_3'' = \ln[\exp(-i\varphi)\cosh\theta + \sqrt{\exp(-2i\varphi)\cosh^2\theta - 1}]$, and θ is a select value $\leq \frac{\pi}{2}$. The contour must now be connected from P_3 to P_2, and P_2 in the complex $\theta' + i\theta''$ plane is given by

$$\theta_2' + i\theta_2'' = \frac{\pi}{2} + i(\xi' + i\xi'') ,$$

or

$$\theta_2' = \frac{\pi}{2} - \xi'' ,$$

and

$$\theta_2'' = \zeta' ,$$

provided θ in (2.19) is equal to zero.
Finally, the contour extends to the infinity of the imaginary axis along a contour $\theta' < \frac{\pi}{2}$. The break in the contour between P_1 and P_2 can be taken at a convenient point P_3 corresponding to a zero of the Bessel function $J_o(\beta r \sin\theta_o)$, so that $\theta_o \leq \theta'$. Note that the region between the original contour 0 to $\frac{\pi}{2} + i\infty$ and this new contour is analytic. Alternatively, the points P_1 and P_3 can be projected to the θ' axis, and the contour from 0 to P_o, P_o to P_2, and P_2 to $\theta'' = i\infty$ can also be used. Finally, a contour is followed a short distance 0 to P_4 along the real axis, then along a straight line to P_1, and along an identical contour to P_3, P_2, and the infinity of the imaginary axis. All integration contours tested with the computer program gave identical results within specified accuracy.

It has been demonstrated (Johler, 1969c) that integrals of the type (2.15) involving Bessel functions of real argument (or with relatively small imaginary parts in the argument) can be evaluated as an alternating series in which each term is calculated from a Gaussian quadrature. The zeroes of the Bessel function determine the limits of integration and the turning point for the sign change of the resultant alternating series. Since this technique is the same as the one discussed in an earlier paper

(Johler, 1969c) it will not be repeated here. A complete computer program for (2.15) is discussed in the appendix. This program uses the technique of continuous stratification illustrated in figure 1. The computer subroutine for calculating $T_{\bullet\bullet}$ was, of course, required to accommodate complex angles of incidence $\varphi_1 = \theta$. The theoretical basis of this subroutine is discussed elsewhere (Johler 1967). The complexity of the terrestrial magnetic field has, obviously, been removed from the program, since this analysis is concerned with an isotropic plasma.

3. DISCUSSION AND CONCLUSIONS

The ground wave was calculated from (2.12) and compared with the classical ground wave computer calculation (Johler, 1969b; Johler and Morganstern, 1965) over both plane and spherical ground. At distances greater than about 200 km the spherical correction may of course become significant. However, at the distances we are concerned with here the plane ground error was a fraction of a decibel in the amplitude. The computer program described in section 5 which evaluates (2.13) was then used in conjunction with the profile given in figure 1, together with the independent variable F_n. Note that the production rate is related to the square of this factor, $q \propto F_n^2$, according to (1.2). Values of F_n from 0.1 to 40, which in this author's estimate represent all physically possible values resulting from fallout, were then introduced.

The most notworthy feature of the results obtained in figure 4 is a decrease in the amplitude of the propagated wave relative to the normal ground wave for values of F_n of interest to this problem. This is physically a consequence of the fact that the propagated energy is slightly absorbed by the ions near the surface of the ground. If the atmosphere were uniformly ionized, the wave would be much more

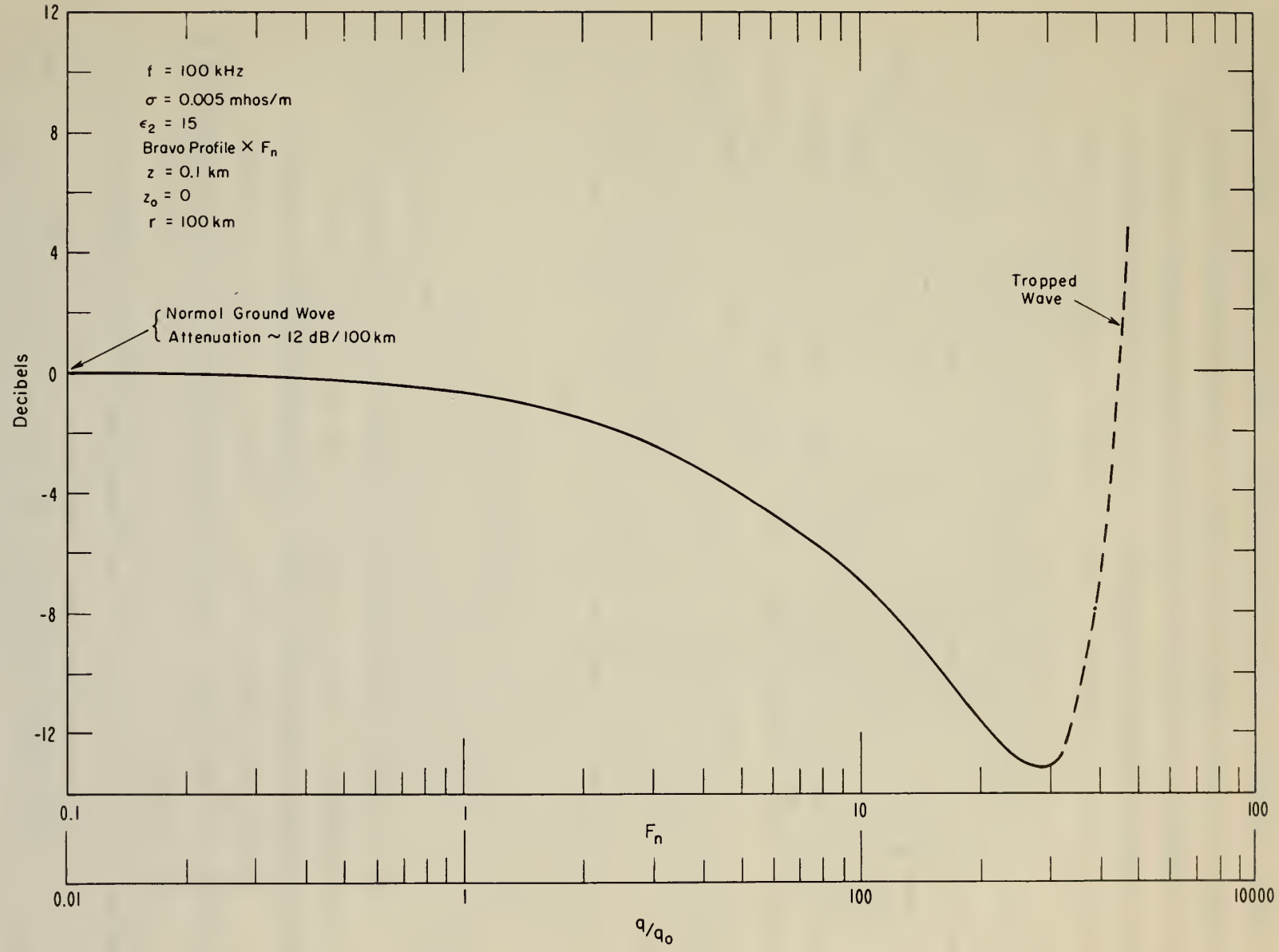

Figure 4. Amplitude of the calculated vertical electric field as a function of the independent variable, F_n, i.e., the profile multiplier, at a frequency of 100 kHz and a distance of 100 km.

severely absorbed as F_n was increased (Johler 1969b). Since the atmosphere contains only a thin film of ionization near the ground, the wave propagates through the air but is concentrated near the ground. This is true at least for values of F_n up to 20. At this point, the attenuation has increased to 12 dB relative to the normal ground waves, which would be equivalent to increasing the production rate by a factor of 400 with respect to the original BRAVO model, $F_n = 1$. The possibility of such extreme production rates does not seem likely, but if it were possible to increase the number density of the BRAVO profile to $F_n = 40$ there would be a tendency toward excitation of a trapped wave in the ionized atmosphere. This would cause an enhancement of the field. Also, the attenuation of the normal ground wave as a function of distance at a steady 12 dB / 100 km would be replaced by a standing wave as a function of distance. It would therefore seem that the 12 dB attenuation at a distance of 100 km is a reasonable maximum attenuation for physically possible values of F_n applied to the BRAVO model.

4. REFERENCES

AEC (1962), The effects of nuclear weapons, U. S. Atomic Energy Commission (U. S. Govt. Printing Office, Washington, D. C. 20402).

Brekhovskikh, L. M. (1960), Waves in Layered Media (Academic Press, New York, N. Y.).

Brueckner, K. A. (1964), Ion-Ion recombination, J. Chem. Phys. 40, 439-444.

Budden, K. G. (1961), The Wave-Guide Mode Theory of Wave Propagation (Prentice-Hall, Inc., Englewood Cliffs, N. J.).

Hirsh, N. M. (1967), VLF studies in simulated sub-D region, G. C. Dewey Corporation, 331 East 38th St., New York, N.Y.

Johler, J. R. (1967), Theory of propagation of low frequency terrestrial radio waves--mathematical techniques for the interpretation of D-region propagation studies, ESSA Tech. Rept. IER 48-ITSA 47 (U. S. Govt. Printing Office, Washington, D. C. 20402).

Johler, J. R. (1969a), Ground wave propagation in a normal and an ionized atmosphere, ESSA Tech. Rept. ERL 121-ITS 85 (U. S. Govt. Printing Office, Washington, D. C. 20402).

Johler, J. R. (1969b), Loran C,D phase corrections over irregular, inhomogeneous terrain-simplified computer methods, ESSA Tech. Rept. ERL 116-ITS 83 (U. S. Govt. Printing Office, Washington, D. C. 20402).

Johler, J. R. (1969c), Mutual impedance of loop antennas over finitely conducting ground, ESSA Tech. Rept. ERL 122-ITS 86 (U. S. Govt. Printing Office, Washington, D. C. 20402).

Johler, J. R., and J. D. Harper, Jr. (1962), Reflection and transmission of radio waves at a continuously stratified plasma with arbitrary magnetic induction, J. of Res. NBS 66D (Radio Prop.) No. 1, 81-99.

Johler, J. R., and L. A. Berry (1965), On the effect of heavy ions on LF propagation, with special references to a nuclear environment, NBS Tech. Note 313 (U. S. Govt. Printing Office, Washington, D. C. 20402).

Johler, J. R., and J. C. Morgenstern (1965), Propagation of the ground wave electromagnetic signal with particular reference to a pulse of nuclear origin, Proc. IEEE 53, No. 12, 2043-2053.

Loeb, L. B. (1961), Basic Processes of Gaseous Electronics (University of California Press, L. A.).

Natanson, G. L. (1959), The theory of volume recombination of ions, Zhurnal Technicheskoe Fiziki 29, No. 11, 1373-1380 (English trans. Soviet Phys. Tech. Phys. 4, 1263-1269, 1959).

Rutherford, E. (1913), Radioactive Substances and Their Radiation (Cambridge at the University Press).

Sayers, J. (1938), Ionic recombination in air, Proc. Roy. Soc. (London) A169, 83.

Sommerfeld, A. (1909), Über die Ausbreitung der Wellen in der drahtlösen Telegraphie, Ann. Physik 28, 665.

Sommerfeld, A. (1926), Über die Ausbreitung der Wellen in der drahtlösen Telegraphie, Ann. Physik 81, 1135.

Thomson, J. J. (1906), Conduction of Electricity Through Gases (Cambridge at the University Press).

Thomson, J. J. (1924), Recombination of gaseous ions, the chemical combination of gases and monomolecular reactions, Phil. Mag. s6, 47, No. 278, 337-379.

Thomson, J. J., and G. P. Thomson (1933), Conduction of Electricity Through Gases II (Cambridge at the University Press).

Weyl, H. (1919), Ausbreitung elektromagnetischen Wellen über einem ebenen Leiter, Ann. Physik 60, 481-500.

APPENDIX

Computer Program

The computer program GIDSPAC3 shown in the computation plan, figure 5, calculates the vertical electric field E by means of (2.15). The program has two independent variables, the distance DIST and the profile multiplier F_n = PROMLT. The amplitude $|E|$ V/m in decibels, the phase Arg (E) in radians, and the phase correction in radians,

$$\varphi_c = -\frac{\omega}{c} r - \text{Arg}(E) \text{ (radians)} \tag{5.1}$$

are given, where the field, E, is defined by

$$E = |E| \exp[i\omega t - i\frac{\omega}{c} r - i\varphi_c] . \tag{5.2}$$

Homogeneous waves EZHA, EZHP, PHIC1 and inhomogeneous waves EZIHA, EZIHP, PHIC2 are given separately for convenience, together with the total field, EZA, EZP, PHIC3. Appropriate comments explain each step in the program. A feature of the program is the shift in the integration contour shown in figure 3, which tests the precision of the numerical analysis and interpolation routines used. The shift can be controlled. Thus, in (2.17), φ = AK1P, and with AK1P = 0, the contour 0, P_4, P_o, P_2 to $i\infty$ is followed. With AK1P = AK1P, the contour 0, P_4, P_1, P_3, P_2 to $i\infty$ is followed. Another example would be AK1P = AK1P/2, which would follow a contour between the above contours up to the point P_2. The contour from P_2 to $i\infty$ is never disturbed since it has been optimized according to (2.18).

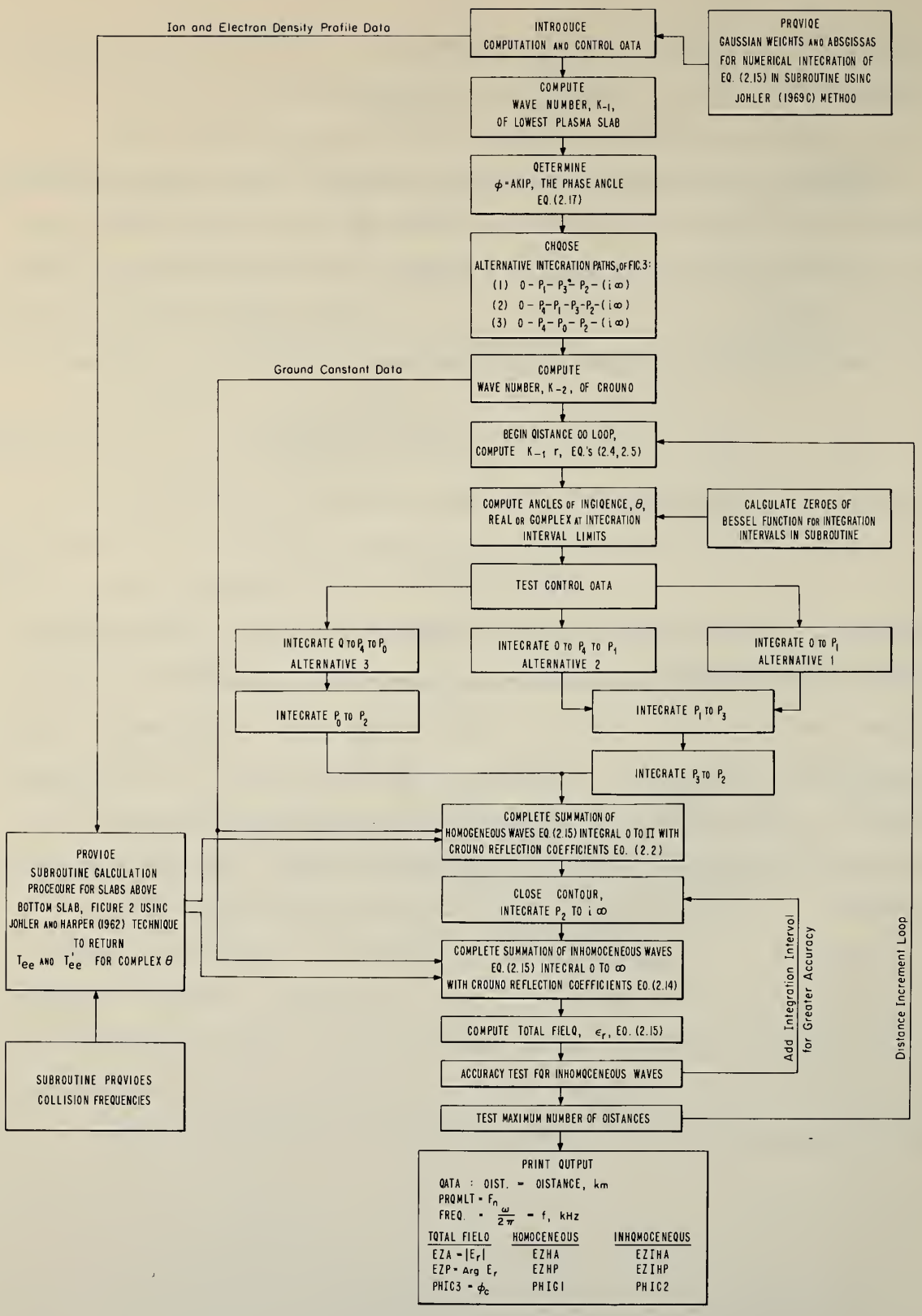

Figure 5. Conceptual plan of program GIDSPAC3.

GPO 858 - 372